ELSEVIER

International Journal of Mass Spectrometry 223–224 (2003) 547–560

International Journal of Mass Spectrometry

www.elsevier.com/locate/ijms

Bond-forming reactivity between CF_3^{2+} and H_2/D_2

Nurun Tafadar, Stephen D. Price*

Chemistry Department, University College London, 20 Gordon Street, London WC1H 0AJ, UK

Received 7 January 2002; accepted 10 June 2002

Abstract

The ionic products formed in collisions of CF_3^{2+} with X_2 (X = H, D) are quantified as a function of the collision energy. The investigations show that, for both neutral targets, the cross-section for forming CF_2^+ ions from electron-transfer reactions and the cross-section for the chemical reaction forming XCF_2^+ increase with decreasing collision energy. This energy dependence is well reproduced by a model based on Landau–Zener theory, as are the markedly differing energy dependencies of the other reaction cross-sections which are available in the literature for molecular dication electron-transfer reactions with X_2. The differing radial velocities at the curve crossing between reactant (dication+neutral) and product (monocation+X_2^+) potentials at a given collision energy is proposed as a possible explanation for the intermolecular isotope effect that has been detected in such electron-transfer reactions. The ratio of the cross-sections for the chemical and electron-transfer reactions following collisions of CF_3^{2+} with X_2 is similar in both of the collision systems and does not vary strongly with energy. A simple model, again employing Landau–Zener theory and requiring the ab initio calculation of the structure and energetics of HCF_2^{2+}, appears to qualitatively account for this energy dependence. Following collisions of CF_3^{2+} with X_2 an additional "chemical" channel, forming XF^+, is also detected. The markedly differing energy dependence of the cross-section for forming XCF_2^+ and XF^+ appear to indicate that these ions are formed via independent pathways. (Int J Mass Spectrom 223–224 (2003) 547–560)

Keywords: Dication; Electron transfer; Chemical reaction; Isotope effect; Collision

1. Introduction

Small molecular doubly charged ions (dications) are usually highly energy-rich and reactive metastable species [1–4]. However, despite their high internal energy content, several molecular dications have recently been shown to display considerable chemical (bond-forming) reactivity with neutral species [4–15]. Initial studies of the "chemical" reactions of molecular dications were prompted by the mass-spectrometric detection of products which involved the formation of new chemical bonds following dication–neutral encounters [11,16]. Detailed studies of the dynamics of dication bond-forming reactions have only been performed for a few systems. The most extensively studied reaction being that between CF_2^{2+} and H_2

$$CF_2^{2+} + H_2 \rightarrow HCF_2^+ + H^+ \quad (1)$$

and the available data on this prototypical two-body reaction has been recently summarised [7]. Specifically, in early experiments the collision energy dependence of the yield of this reaction with H_2 and D_2 was monitored [10]. Subsequently, angular scattering experiments showed that the HCF_2^+ product was primarily forward scattered and that the Coulomb repulsion between the products plays a dominant role in

* Corresponding author. E-mail: s.d.price@ucl.ac.uk

1387-3806/02/$ – see front matter
PII S1387-3806(02)00877-1

the reaction dynamics [5,15]. Some experimental evidence for a short-lived collision complex was obtained and a potential surface model was developed to explain the competition of the various product channels (non-dissociative and dissociative electron-transfer, non-dissociative and dissociative chemical reaction) in dication–neutral collision systems [5]. Following this study, the competition between the two possible bond-forming pathways (yielding HCF_2^+ and DCF_2^+) following collisions of CF_2^{2+} with HD was monitored as a function of collision energy [9]. These experiments showed a strong intramolecular isotope effect favouring the formation of DCF_2^+.

The reaction dynamics of the electron-transfer and bond-forming channels following collisions of CO_2^{2+} with D_2 has also received detailed experimental attention. Specifically, the angular scattering in this collision system has recently been studied [6] as have the intramolecular isotope effects in the reaction of CO_2^{2+} with reactions with HD [7]. For the dominant bond-forming channel

$$CO_2^{2+} + D_2 \rightarrow DCO^+ + D^+ + O \quad (2)$$

the angularly resolved investigation showed that DCO^+ is formed by dissociation of DCO_2^+ and the $DCO_2^+$is formed via a short-lived intermediate $[CO_2–D_2]^{2+}$, which the angular scattering indicates lives for a few tenths of a picosecond at a collision energy of 2.5 eV [6]. The absolute cross-sections also indicated little variation in the yields of the electron-transfer and bond-forming processes with collision energy. However, the cross-section for both these processes was approximately a factor of two larger for collisions with H_2 than collisions with D_2. Recent studies of the intramolecular isotope effects in the chemical reaction of CO_2^{2+} with HD again indicted a strong preference for the formation of DCO^+ [7].

Stimulated by the interesting dynamics and reactivity revealed in these previous studies of dicationic chemistry, this article presents a study of the reactivity of CF_3^{2+} with X_2 (X = H or D). A bond-forming reaction generating XF_2^+ was observed following such encounters in an early overview [11] of dicationic reactivity with small molecules:

$$CF_3^{2+} + X_2 \rightarrow XCF_2^+ + [X + F]^+ \quad (3)$$

However, following this initial observation these precise reactive systems have not been investigated in any greater detail. However, the reactivity of the isotopically related collision system, involving the interaction of CF_3^{2+} with HD, has recently been investigated [7]. These experiments showed a strong intramolecular isotope effect in reaction (3) favouring the formation of DCF_2^+ over HCF_2^+. This intramolecular effect was interpreted as arising from statistical effects affecting the breakdown of an intermediate complex formed upon initial co-ordination of the dication to the neutral [7]. In addition, this recent work detected the formation of small quantities of XF^+ from this collision system. Surprisingly, in contrast to the channel forming XCF_2^+, the formation XF^+ appeared not to exhibit any significant isotope effect.

Other investigations [17,18] of the collisional reactivity of CF_3^{2+} have shown its propensity to lose one neutral fluorine atom, which appears to be weakly bound, to form CF_2^{2+}. This neutral-loss reactivity was interpreted to indicate a C_{2v} dicationic structure, a proposition that has now been supported by theoretical investigations [19,20].

In this paper, we report the results of an investigation of the chemistry following collisions of CF_3^{2+} with X_2. We show that for both neutral targets, over the collision energies studied, the cross-sections for forming both CF_2^+ and XCF_2^+ increase with collision energy and the cross-section for the chemical reaction is comparable with the dissociative electron-transfer cross-section. An additional chemical channel forming XF^+ is also detected.

2. Experimental

The apparatus used in these investigations has been described in detail before [8–10,17]. Briefly the molecular dication of interest is mass selected, using a velocity filter, from the positive ions produced by an electron impact ionisation source. To produce the

CF_3^{2+} dications, we utilise the dissociative double ionisation of CF_4 by ~150 eV electrons. Electrostatic optics are employed to extract the ions from the source and transport them to a velocity filter where mass selection of the appropriate dications to form a beam is performed. The experiments reported in this paper were carried out at low collision energies to maximise the yield of the bond-forming reaction. Hence, after traversing the velocity filter at 500 eV in the laboratory-frame, the kinetic energy of the dications must be substantially reduced before they encounter the neutral molecules. Deceleration of the dication beam is achieved using further ion optics with subsequent refocusing. This procedure results in a dication beam of 1–500 pA at laboratory-frame energies of 2–20 eV. On leaving the decelerator, the dication beam intersects an effusive beam of the neutral collision partner in a collision region, which doubles as the source region of the time of flight mass spectrometer (TOFMS). Product ions formed following the interaction of the molecular dication with the neutral target, in addition to unreacted dications, are periodically (50 kHz) extracted, perpendicular to both the original direction of the dication beam and the neutral gas jet, from the interaction region by pulsing the repeller plate of the TOFMS. The TOFMS is of the standard Wiley and McLaren [21] design and ions reaching the end of the drift tube are accelerated to hit a multichannel plate detector. The pressure of the neutral collision partner is carefully controlled to ensure single collision conditions exist in the interaction region. This is confirmed by the linear dependence of the product ion yields on the number density of the neutral target. Sections of typical TOF mass spectra, illustrating the ionic products of interest, are shown in Fig. 1.

The signals of interest in the product ion mass spectra are those which result from bimolecular encounters. Mass spectra of the ions present in the interaction region in the absence of the collision gas are also recorded. These spectra are used to correct the spectra recorded in the presence of the collision gas to leave only the signals which are due to the bimolecular reactions. In practice these corrections are very small [8–10,17].

In this work, the products following collisions between CF_3^{2+} and both H_2 and D_2 were monitored at the centre of mass collision energies from 0.17 to 0.5 eV and 0.19 to 0.77 eV, respectively. As in previous investigations, the centre of mass collision energy is calculated using the initial dication velocity, which

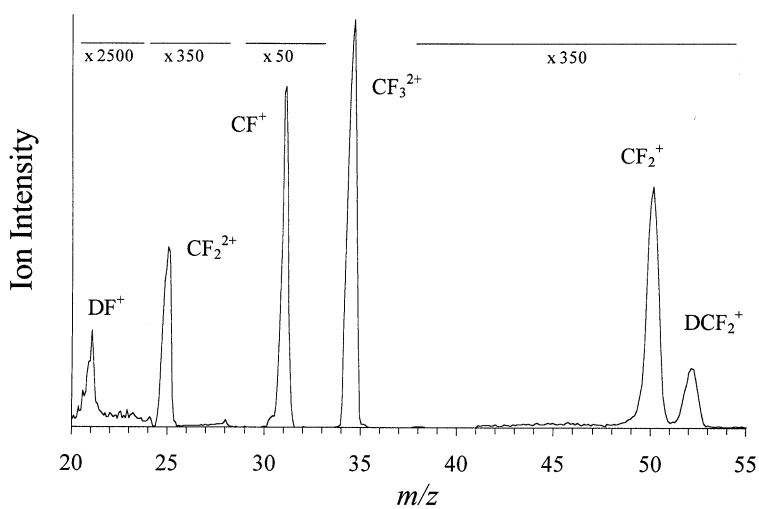

Fig. 1. Sections of a representative mass spectrum recorded following collisions of CF_3^{2+} with D_2 at a laboratory collision energy of 9 eV. As indicated on the figure, the vertical scale is expanded by a variety of factors over certain mass ranges to allow the display of product ion signals of markedly different intensities.

is known from the beam potential, and assuming that the velocity of the neutral molecule is negligible with respect to the velocity of the dication. Given that the neutrals are admitted as an effusive beam and that the dication beams have energies between 4 and 12 eV in the laboratory-frame, this approach is perfectly satisfactory.

3. Results

Time of flight mass spectra were recorded following collisions between CF_3^{2+} and X_2 (X = H, D) at laboratory-frame collision energies in the range 3–12 eV. After correction for any impurity ions present, as described before, these spectra show the presence of X^+, X_2^+, CF_2^{2+}, CF_2^+, CF^+, CF_3^+, XCF_2^+ and XF^+ product ions. Due to the absence of any "real" F^+ signals in our mass spectra, the formation of the CF_n^+ (n = 1–3) ions are readily assigned to dissociative and non-dissociative electron-transfer reactions of CF_3^{2+}:

$$CF_3^{2+} + X_2 \rightarrow CF_n^+ + (3-n)F + [2X]^+ \quad (4)$$

The electron-transfer reactivity of CF_3^{2+} has been discussed extensively in the literature [17] and will not be considered in detail here. Similarly, the neutral-loss reaction forming CF_2^{2+}

$$CF_3^{2+} + X_2 \rightarrow CF_2^{2+} + F + X_2 \quad (5)$$

has been previously identified as a common decay mechanism for perfluorinated dications when they receive electronic or vibrational excitation (either in a collision or by photoexcitation) [17,18,22,23]. Hence, we will focus in this investigation on the bond-forming reactivity in this system, which forms XCF_2^+ and XF^+.

The XCF_2^+ ion has been identified before as a product of collisions of CF_3^{2+} with H_2, although no dynamical information was obtained from this simple mass-spectrometric experiment [11]. Indeed, even the simple mass-spectrometric observations from our current experiments provide additional information on the identity of the ion pair formed by the chemical reaction producing HCF_2^+ (Eq. (3)). Specifically, reaction (3) could produce XCF_2^+ together with either F^+, XF^+ or X^+ ions. However, the absence of any bimolecular F^+ signals in our mass spectra, and the fact that the XF^+ signal is considerably weaker than the XCF_2^+ signal, strongly indicates that $HCF_2^+ + X^+ + F$ are the products of reaction (3). A conclusion in agreement with the recent investigation of the reactivity of CF_3^{2+} with HD [7].

As mentioned before, the formation of XF^+ has recently been detected in a series of experiments to study intramolecular isotope effects in the reaction of CF_3^{2+} with HD [7]. Interestingly, no intramolecular isotope effect appeared in the XF^+ product ion yield, in contrast to the XCF_2^+ channel. This difference was thought to indicate that the XF^+ is formed via a markedly different reaction mechanism to XCF_2^+. As can be seen from Fig. 1, the signals due to the XF^+ and XCF_2^+ ions are clearly visible in our spectra and the intensities of the product ions of interest were recorded as a function of collision energy. For all but HCF_2^+ these product ion intensities can be determined simply by summing the counts in the channels making up the peak and applying a correction for the non-zero background underlying the ion peaks. For the HCF_2^+ product, which is imperfectly resolved at the baseline level from the neighbouring CF_2^+ signal, a peak fitting procedure was used to determine this ions relative intensity. For all these signals the contribution from the "impurity ions" present when the neutral gas is absent, either transmitted by the velocity filter or generated in collisions with residual gas, is small (<5%). The product ion intensities I determined in the above-mentioned manner for collisions with H_2 and D_2 are displayed as a function of collision energy in Tables 1 and 2. Note that these individual intensities, in a change from our previous investigations [7–10,17], are expressed in arbitrary units relative to the unreacted dication intensity. We term this ratio of the product ion intensity relative to the unreacted diction intensity, $I(CF_2^+)/I(CF_3^{2+})$, the *absolute product ion yield*. Since we operate under single collision conditions [24], the unreacted dication intensity is equal within experimental uncertainty to the

Table 1
Absolute product ion yields $I(A^+)/I(CF_3^{2+})$, correction factors α and the resulting corrected absolute product ion yields $R(A^+)/R(CF_3^{2+})$ for the formation of CF_2^+ and DCF_2^+ from collisions of CF_3^{2+} with D_2 as a function of laboratory collision energy E_{lab}

E_{lab} (eV)	E_{COM} (eV)	$10^3(I(CF_2^+)/I(CF_3^{2+}))$	$\alpha(CF_2^+/CF_3^{2+})$	$10^3(R(CF_2^+)/R(CF_3^{2+}))$	$10^3(I(DCF_2^+)/I(CF_3^{2+}))$	$\alpha(DCF_2^+/CF_3^{2+})$	$10^3(R(DCF_2^+)/R(CF_3^{2+}))$
4.0	0.22	3.58	2.20	7.87	1.16	1.89	2.19
5.0	0.27	2.84	2.07	5.89	0.99	1.80	1.78
6.0	0.33	3.15	1.97	6.20	1.01	1.72	1.74
7.0	0.38	1.53	1.89	2.90	0.47	1.65	0.78
8.0	0.44	2.24	1.82	4.08	0.69	1.60	1.11
9.0	0.49	1.78	1.77	3.15	0.50	1.56	0.78
10.0	0.55	1.56	1.73	2.71	0.44	1.52	0.66
11.0	0.60	2.04	1.70	3.47	0.52	1.49	0.78
12.0	0.66	2.76	1.69	4.67	0.73	1.48	1.09

The yields are presented in arbitrary units as discussed in the text. The centre of mass collision energy E_{COM} is also given.

incident dication current. In addition, all the experiments with a given neutral target were performed at the same neutral gas pressure. Hence, when corrected for any discrimination effects (see following sections), these absolute yields should be proportional to the absolute cross-section for forming the individual product ions. Such corrected absolute product ion yields thus display the energy variation of the cross-sections for forming individual product ions. In previous studies, we expressed our results as a ratio of the intensities of pair of product ions [7–10,17] and could only observe relative variations in the product ion yields with collision energy. Hence, this new data treatment provides more fundamental information on the reactivity of a given dication collision system.

The increased information provided by the absolute ion yields comes at a small price, as there are additional sources of uncertainty in these data in comparison to the relative product ion intensities presented in earlier work. Due to the focussing of the TOFMS any unreacted dications arrive in a 30 ns time window, a time spread comparable with the dead time of our timing electronics. Hence, if the dication beam is sufficiently intense there is a possibility of "missing" some dication arrivals in the dead time of the electronics. However, within each set of experiments, one set with D_2 and one set with H_2, the dication beam current was approximately constant. Hence, the constant of proportionality between the dication counts in the spectrum and the dication beam intensity will be

Table 2
Absolute product ion yields $I(A^+)/I(CF_3^{2+})$, correction factors α and the resulting corrected absolute product ion yields $R(A^+)/R(CF_3^{2+})$ for the formation of CF_2^+ and HCF_2^+ from collisions of CF_3^{2+} with H_2 as a function of laboratory collision energy E_{lab}

E_{lab} (eV)	E_{COM} (eV)	$10^3(I(CF_2^+)/I(CF_3^{2+}))$	$\alpha(CF_2^+/CF_3^{2+})$	$10^3(R(CF_2^+)/R(CF_3^{2+}))$	$10^3(I(HCF_2^+)/I(CF_3^{2+}))$	$\alpha(HCF_2^+/CF_3^{2+})$	$10^3(R(HCF_2^+)/R(CF_3^{2+}))$
4.0	0.11	3.43	2.00	6.85	1.28	1.78	2.28
5.0	0.14	2.75	1.89	5.20	1.02	1.69	1.73
6.0	0.17	2.56	1.80	4.61	0.91	1.62	1.48
7.0	0.20	2.62	1.73	4.52	0.93	1.56	1.46
8.0	0.23	2.15	1.67	3.60	0.72	1.51	1.08
9.0	0.25	2.29	1.62	3.71	0.78	1.47	1.15
10.0	0.28	2.33	1.58	3.68	0.73	1.44	1.05
11.0	0.31	2.14	1.55	3.31	0.68	1.41	0.95
12.0	0.34	1.71	1.53	2.62	0.57	1.39	0.79

The yields are presented in arbitrary units as discussed in the text. The centre of mass collision energy E_{COM} is also given.

approximately the same for each set of experiments. Thus, with the addition of some extra uncertainty, we can ratio the product ion intensities to the dication counts to produce absolute yields which reproduce the trends in the absolute cross-sections for forming each product ion of interest. It is important to note that these absolute yields are not quantitatively comparable between the H_2 and D_2 data. This is because significantly different beam currents were used for these two sets of experiments, due to different focussing conditions being employed in the H_2 experiments to achieve higher resolution in the TOFMS, and hence the constant of proportionality between the dication counts in the spectrum and the dication beam intensity will be different between the H_2 and D_2 experiments.

4. Product ion intensities

Before interpreting the absolute yields we measure (Tables 1 and 2) we must be sure our experimental absolute product ion yields accurately reflect the relative cross-sections for forming the ions of interest. Specifically, we must correct for any mass discrimination between the relevant ions which exists in our experiment. As has been discussed intensively before [8–10,17], if ions of interest possess markedly different transverse kinetic energies across the source region of our TOFMS, then those ions with larger transverse kinetic energies in the laboratory-frame will travel a greater distance away from the central axis of the TOFMS than any less energetic ions. Hence, a proportion of the more energetic ions may miss the detector. To correct for this effect, we calculate the length of the interaction region that is imaged onto the ion detector for ions of different transverse energies. This correction procedure, which is described in the following sections, produces relative ion intensities which agree satisfactorily with other quantitative measurements of the product ion yields in dication neutral collisions, where such measurements are available [5,10,15].

The transverse velocity of the reactant dications is known from the beam energy. The transverse velocity of the product ions in the laboratory-frame can be calculated, given the value of the kinetic energy release (KER) for the reaction and the laboratory-frame collision energy, using basic kinematics. However, no data concerning the values of the KER for the chemical reaction between CF_3^{2+} and X_2 are available in the literature. However, for related collision systems such data is available. For the reaction between CO_2^{2+} and X_2, recent work [6] shows the DCO^+ product from $CO_2^{2+} + D_2$ is predominantly, although by no means exclusively, forward scattered with a KER centred around 5–7 eV. The most probable KERs for the formation of DCO_2^+ and CO_2^+ in this collision system are also of similar magnitude. Product ion KER distributions have also been determined for the bond-forming channel in the CF_2^{2+}/D_2 collision system [5] again showing a most probable energy release around 7 eV. Given the above information, we have used a KER value of 7 eV to estimate the detection efficiency of XCF_2^+ and CF_2^+ in our experiments. It is important to note that the correction factors we calculate are not a strong function of the KER. Hence, taking a value of the KER from other experiments is not a major approximation. Given a value for the KER, the derivation of a product ion correction factor for our experiments has been presented in detail before [10]. Briefly, to use these representative KER values to determine the average product ion velocity we assume that the dynamics of the collision system predominantly involve forward scattering. Again, this is an assumption, but the two angularly resolved investigations of dication reactivity indicate that forward scattering is the dominant scattering direction in dication chemical reactions [5,6]. In fact, calculating the relative discrimination using forward scattering provides an upper limit on the potential experimental discrimination.

To form XCF_2^+, we assume, as has been shown to be true for the formation of HCO^+ from collisions of CO_2^{2+} with X_2, that the KER is distributed in a charge separating two-body reaction forming $X^+ + XCF_3^+$, and no neutral species are lost (e.g., $XCF_3^+ \rightarrow XCF_2^+ + F$) until the two ions are well separated [6]. Again this provides a "worst case" estimate of our discrimination.

Table 3
Relative product ion yields $I(A^+)/I(CF_2^+)$, correction factors α and the resulting corrected product ion yields $R(A^+)/R(CF_2^+)$ for the formation of XCF_2^+ from collisions of CF_3^{2+} with X_2 (X = H, D) as a function of laboratory collision energy E_{lab}

E_{lab} (eV)	$CF_3^{2+} + D_2$				$CF_3^{2+} + H_2$			
	E_{COM} (eV)	$(I(DCF_2^+)/I(CF_2^+))$	$\alpha(DCF_2^+/CF_2^+)$	$(R(DCF_2^+)/R(CF_2^+))$	E_{COM} (eV)	$(I(HCF_2^+)/I(CF_2^+))$	$\alpha(HCF_2^+/CF_2^+)$	$(R(HCF_2^+)/R(CF_2^+))$
4.0	0.22	0.32	0.86	0.28	0.11	0.37	0.89	0.33
5.0	0.27	0.35	0.87	0.30	0.14	0.37	0.90	0.33
6.0	0.33	0.32	0.87	0.28	0.17	0.35	0.90	0.32
7.0	0.38	0.31	0.87	0.27	0.20	0.36	0.90	0.32
8.0	0.44	0.31	0.88	0.27	0.23	0.33	0.91	0.30
9.0	0.49	0.28	0.88	0.25	0.25	0.34	0.91	0.31
10.0	0.55	0.28	0.88	0.24	0.28	0.31	0.91	0.28
11.0	0.60	0.26	0.88	0.23	0.31	0.32	0.91	0.29
12.0	0.66	0.27	0.87	0.23	0.34	0.34	0.91	0.30

The centre of mass collision energy E_{COM} is also given.

We use this representative KER values to evaluate the respective ion velocities $v(P^+)$ for the relevant product ions and determine the reactant dication velocity $v(CF_3^{2+})$ from the energy of the dication beam. We also determine, from the geometry of the TOFMS, the different lengths of the ion source, $L(P^+)$ for the product of interest and $L(CF_3^{2+})$ for the dication, which are imaged onto the detector for ions of the given velocities. Given these lengths and velocities, we can derive the following relation to determine the corrected absolute product ion yields $R(P^+)/R(CF_3^{2+})$ by scaling the experimentally measured absolute product ion yields $I(P^+)/I(CF_3^{2+})$:

$$\frac{R(P^+)}{R(CF_3^{2+})} = \frac{L(CF_3^{2+})}{L(P^+)} \frac{v(P^+)}{v(CF_3^{2+})} \frac{I(P^+)}{I(CF_3^{2+})} = \alpha \left(\frac{P^+}{CF_3^{2+}} \right) \frac{I(P^+)}{I(CF_3^{2+})} \quad (6)$$

The corrected absolute product ion yield should be proportional to the absolute cross-section for forming the relevant product. The correction factors $\alpha(P^+/CF_3^{2+})$ we derive (Tables 1 and 2) vary more significantly than those we determine when compensating for the relative discrimination between two product ions. This larger variation in α is due to the more significant differences between the energies of a product ion and a reactant dication, than between a pair of ionic products. This is demonstrated in Table 3 and Fig. 3 where we show the variation with collision energy of the relative product ion intensities between the bond-forming and electron-transfer channels (XCF_2^+ and CF_2^+) which can be compared with analogous values we have derived for other dication collision systems in earlier work [8–10,17]. Note that the values of $R(XCF_2^+)/R(CF_2^+)$ presented in Table 3 are derived by averaging ratios derived from each individual mass spectrum, followed by appropriate correction. Hence, these values are more accurate than those one would obtain from the ratio of the values of $R(XCF_2^+)/R(CF_3^{2+})$ and $R(CF_2^+)/R(CF_3^{2+})$ presented in Tables 1 and 2, although the later values show an identical trend.

The correction of the XF^+ intensities for product ion energy effects is problematical. Hence, in Table 4 we present just the raw intensity ratios of XF^+ to the dication signal and the ratio of the uncorrected XF^+ signal to the corrected dication signal. This subject is discussed in some detail below.

5. Discussion

The corrected absolute product ion yields in arbitrary units for forming XCF_2^+ and CF_2^+ from collisions between CF_3^{2+} and X_2 are listed in Tables 1 and 2 and displayed in Fig. 2. Note that, as explained before, due to the different dication beam conditions

Table 4
Absolute product ion yields $I(A^+)/I(CF_3^{2+})$ and the resulting yield $I(A^+)/R(CF_3^{2+})$, when corrected for the variation in the efficiency of dication detection with collision energy, for the formation of XF^+ from collisions of CF_3^{2+} with X_2 (X = H, D) as a function of laboratory collision energy E_{lab}

E_{lab} (eV)	$10^5(I(DF^+)/I(CF_3^{2+}))$	$10^5(I(DF^+)/R(CF_3^{2+}))$	$10^5(I(HF^+)/I(CF_3^{2+}))$	$10^5(I(HF^+)/R(CF_3^{2+}))$
4.0	5.68	2.05	5.23	1.96
5.0	6.04	2.14	7.20	2.63
6.0	8.25	2.88	5.48	1.97
7.0	4.65	1.61	5.83	2.08
8.0	7.88	2.69	6.27	2.21
9.0	6.22	2.12	8.61	3.01
10.0	6.37	2.14	8.26	2.86
11.0	9.48	3.19	11.74	4.05
12.0	12.98	4.34	8.10	2.80

The yields are presented in arbitrary units as discussed in the text.

existing in the two sets of experiments, with H_2 and with D_2, the corrected yields $R(XCF_2^+)/R(CF_3^{2+})$ and $R(CF_2^+)/R(CF_3^{2+})$ are not in principle directly comparable between the H_2 and D_2 experiments. However, qualitatively the corrected yields seem similar for the two systems. For both systems, the absolute yields of the major chemical product (XCF_2^+) and the electron-transfer product CF_2^+ increase with decreasing collision energy. This trend, although accentuated by the correction for the translational energies of the relevant ions, is clearly visible in the raw data (Tables 1 and 2). Obviously, as discussed before, some additional uncertainty is introduced due to the more significant differences in the collection efficiency between an energetic product ion and the slower reactant dication, as compared with a pair of product ions. However, since the trend in the corrected data and in the uncorrected data remain the same, we feel confident this is a real phenomenon. Indeed, the good agreement between relative ion yields derived from our experiments and work from other laboratories supports the validity and accuracy of the correction procedure [5,10,15].

The scale of the increase seems similar for both the D_2 and the H_2 collision systems and the ratio of the bond-forming yield to the electron-transfer yield is similar in both systems (Fig. 2). In fact when the relative yield of XCF_2^+ to CF_2^+ is plotted against the centre of mass collision energy the same relationship appears to be followed for both the H_2 and D_2 data (Fig. 3). We discuss the reasons for this approximately linear relationship between the relative intensities of the products of bond-forming and electron-transfer reactivity, which has been seen before for CF_2^{2+}/X_2 collisions [10], in more detail in the following sections.

The increase in the yield of CF_2^+ (Fig. 2) with decreasing collision energy is reproduced well by a simple Landau–Zener model. This model, which has been described in detail before [25,26], involves calculating the probability for electron transfer as a function of impact parameter from the Landau–Zener equation and then integrating over the impact parameter to yield the electron-transfer cross-section. To use the Landau–Zener equation, we need values for the relative energetics of the product and reactant ions, which are available in the literature [20,27], and a value for the coupling matrix element which we estimate using the model of Olson et al. [28]. As in previous work, we model this dissociative electron-transfer reaction as initially populating excited states of CF_3^+ which subsequently dissociate to CF_2^+. Experimental evidence supports the operation of this sequential pathway [6]. The energetics of the CF_3^+ states dissociating to CF_2^+ are obtained from previous ab initio studies of the electronic structure of CF_3^+ [17]. This investigation revealed that a group of excited electronic states of CF_3^+ with approximately 8 eV of electronic excitation, with respect to the ground state of CF_3^+, dissociate

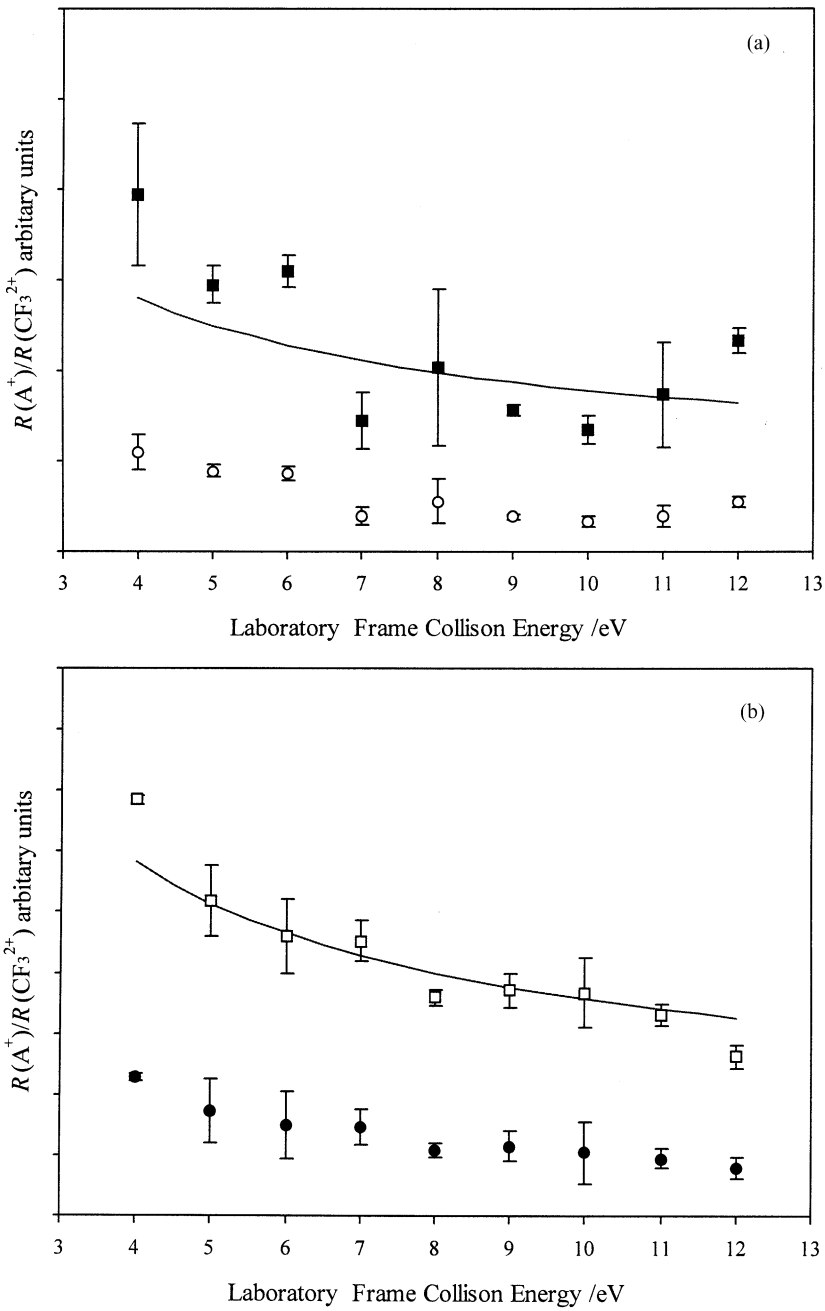

Fig. 2. Variation of the corrected absolute product ion yields $R(CF_2^+)/R(CF_3^{2+})$ and $R(XCF_2^+)/R(CF_3^{2+})$ of CF_2^+ (■, □) and XCF_2^+ (○, ●) following collisions of CF_3^{2+} with X_2 with laboratory collision energy. (a) X = D, (b) X = H. The solid line on each plot is the result of a Landau–Zener calculation of the yield of CF_2^+. See text for details.

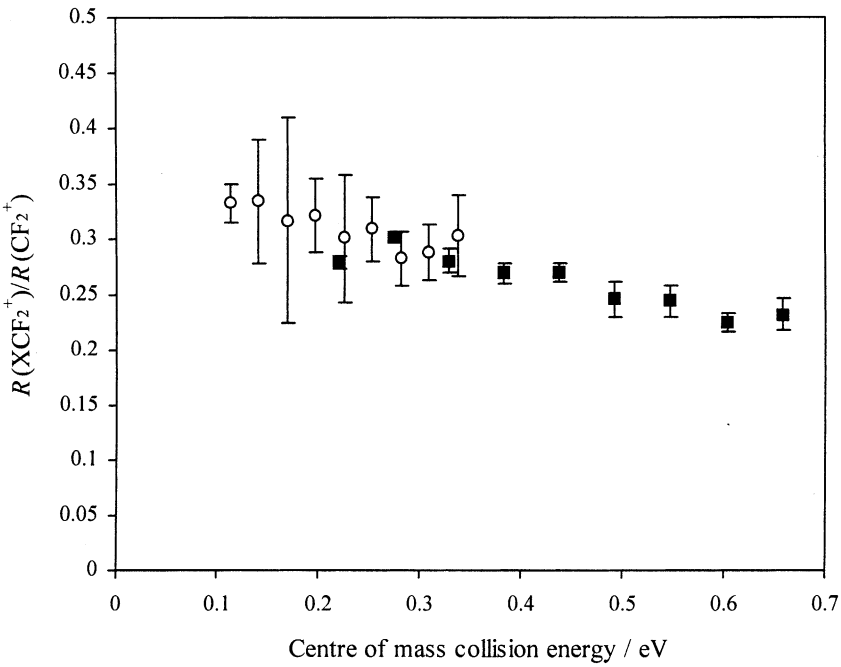

Fig. 3. Corrected relative product ion yields $R(A^+)/R(CF_2^+)$ for the formation of XCF_2^+ from collisions of CF_3^{2+} with H_2 (○) and D_2 (■) as a function of the centre of mass collision energy.

to form CF_2^+. Hence, in our model Landau–Zener calculation we determine the cross-section for populating such states in an electron-transfer reaction. In Fig. 2, the cross-sections derived from the Landau–Zener calculations are normalised to the experimental data, which is in arbitrary units as discussed before, using a single scaling parameter which is derived by minimising the sum of the squares of the deviation between the experimental data and the calculated values. No other fitting, other than this simple scaling to allow for the different units, is used.

The increase, with decreasing collision energy, of the absolute ion yields for electron-transfer with both H_2 and D_2 following collisions with CF_3^{2+} (Fig. 2) is in contrast to the yield of CF_2^+ formed by electron-transfer in the $CF_2^{2+} + X_2$ collision system [5]. In this non-dissociative electron-transfer reaction the yield of CF_2^+ has been shown to fall with decreasing collision energy. Using the available energetics this fall is also well modelled by our (and the authors) Landau–Zener model [5]. The precise behaviour of the electron-transfer cross-section as a function of collision energy in the Landau–Zener model appears to subtly depend on both the strength of the coupling at the crossing and the relative velocity of the reactants.

Recent experiments have also studied the non-dissociative electron-transfer reaction in the $CO_2^{2+} + X_2$ system [6]. This study shows that the yield of CO_2^+ in each collision system is roughly independent of the collision energy and that principally the A and B states of CO_2^+ are populated. We have carried out preliminary Landau–Zener calculations which indicate the energy independence of the CO_2^+ yield is a result of the cancellation of the increase in the cross-section for populating the B state of CO_2^+ with increasing collision energy by the decrease in the cross-section for populating the A state.

Also clearly apparent in the CO_2^{2+}/X_2 data [6] is an intermolecular isotope effect where the absolute cross-section for the formation of CO_2^+ in collisions of CO_2^{2+} with X_2 is approximately a factor of two larger for H_2 than for D_2. Our Landau–Zener model

qualitatively predicts such a preference as, in general, the electron-transfer cross-sections are larger at a given laboratory collision energy for H_2 than for D_2. This isotope effect arises principally from the difference in the radial velocity at the crossing, for a given laboratory collision energy, of the H_2 and D_2 collision systems. Such an effect is also perhaps just apparent in the available absolute cross-sections for the CF_2^{2+}/X_2 systems at lower collision energies [5].

As described before, for collisions with both H_2 and D_2, the relative yields of XCF_2^+ to CF_2^+, when plotted as a function of centre of mass collision energy, seems to lie on the same curve (Fig. 3). Similar behaviour has been observed for the relative yields of bond-forming and electron-transfer reactions in the CF_2^{2+}/X_2 system [10]. To try and understand the source of these relationships we have extended a simple model of the competition between the electron-transfer and reactive channels. A schematic potential energy surface appropriate for this model has been previously developed to qualitatively explain the competition of electron-transfer and chemical reactivity in dication collision systems [5,6] and is shown in Fig. 4. Since non-dissociative reactions are intrinsically less complex than the corresponding dissociative reactions, we have chosen to model the competition between the formation of CF_2^+ and H_2^+ and HCF_2^+ and H^+ following interactions of CF_2^{2+} with H_2. We calculate the probabilities (δ_{et} and δ_{rxn}) for remaining on the diabatic potential at the electron-transfer crossing (crossing 1, Fig. 4) and the "reactive" crossing (crossing 2, Fig. 4) using the Landau–Zener formalism [29–31]

$$\delta = \exp\left(\frac{-\pi^2(H_{12})^2}{|V'_p - V'_r|v_b h}\right) \quad (7)$$

and then use these probabilities, as described below, to estimate the relative probabilities of electron-transfer and chemical reaction. Calculation of δ_{et}, which is a function of impact parameter and collision energy, is straightforward as the energetics of crossing 1 (Fig. 4) are well established [5,15,32]. However, the parameters describing the reactive crossing (crossing 2, Fig. 4) are less well established. The energetics of the singly charged products ($HCF_2^+ + H^+$) are well known [27] but the energetics of HCF_2^{2+} ion are unknown. Hence, we have calculated the ionisation energy to form HCF_2^{2+} from HCF_2^+ using Gaussian 98 [33]. These calculations were performed using an CCS(T)-VTZ basis with an MP2 algorithm to identify the relevant minima of HCF_2^{n+} ($n = 0$–2) and then calculating the energetics at those minima using a CCSD algorithm. Such an approach has been successfully used to characterise dicationic species in previous work [6,7,17,19,20,32,34,35]. For the neutral and singly charged molecules, we find equilibrium geometries

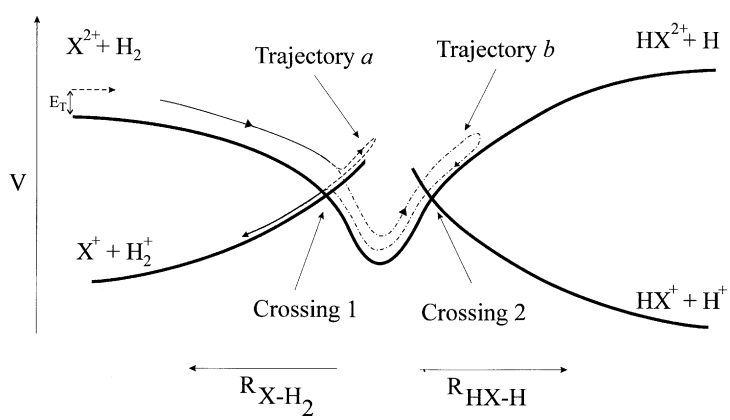

Fig. 4. Schematic potential energy surface to explain the competition of electron transfer and reactivity in dication molecule collisions. Two trajectories (a and b) discussed in the text are illustrated.

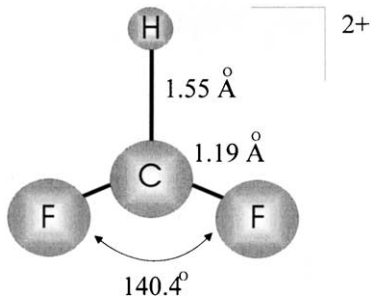

Fig. 5. Calculated geometry of HCF_2^{2+}. The details of the calculations are given in the text.

in good agreement with earlier computational studies of these species [36]. From these minima, we calculate an adiabatic first ionisation potential of HCF_2 of 8.5 eV and a vertical ionisation potential of 10.0 eV, in good agreement with observed values [27]. For the dication, we determine the C_{2v} equilibrium geometry shown in Fig. 5. Our calculated energetics of the dication at this minimum and at the geometry of the neutral and singly charged molecules yield values for the vertical double ionisation energy (35.0 eV), adiabatic double ionisation energy (32.7 eV) and the adiabatic second ionisation energy (24.2 eV), the last value being that of a transition from the equilibrium structure of the monocation to the equilibrium geometry of the dication. This final energy difference, combined with the established energetics of the products, allows us to determine that the exothermicity for $HCF_2^{2+} + H \rightarrow HCF_2^{+} + H^{+}$ is 10.58 eV and that the $HCF_2^{2+} + H$ asymptote lies 3.0 eV above the $CF_2^{2+} + H_2$ asymptote and hence, as predicted [5], is inaccessible at the collision energies employed in previous work.

Using the above-mentioned energetics, we can calculate δ_{rxn} and hence, together with our value of δ_{et}, estimate the probability of the CF_3^{2+}/X_2 collision system leaving the potential energy surface illustrated in Fig. 4 having undergone either electron-transfer or chemical reaction. Given that we are at a centre of mass collision energy which is insufficient to allow access to the $HCF_2^{2+} + H$ asymptote, there are many possible pathways through our schematic potential energy surface which can result in the formation of the electron-transfer or chemical reaction products. For example, an electron-transfer reaction can simply occur via a surface-hopping at crossing 1 followed by a non-crossing as the singly charged ions separate (Trajectory a, Fig. 4). However, more complex pathways are also possible. For example, diabatic passage at crossing 1 followed by two passes of crossing 2 without crossing and finally a surface-hopping when the system returns to crossing 1 (Trajectory b, Fig. 4). Writing an expression for the electron-transfer probability and the chemical reaction probability which includes all possible trajectories results in the expressions below which are a function of the radial velocity at the crossing which depends in turn on the impact parameter and the collision energy

$$p_{rxn} = \delta_{et}(1 - \delta_{rxn}) + \delta_{et}\delta_{rxn}^2 \sum_{i=0}^{\infty} (1 - \delta_{rxn})^{2i+1} \quad (8)$$

$$p_{et} = \delta_{et}(1 - \delta_{et}) + \delta_{et}(1 - \delta_{et})\delta_{rxn}^2 \sum_{i=0}^{\infty} (1 - \delta_{rxn})^{2i} \quad (9)$$

Integrating these expressions over the impact parameter b from zero until the collision just reaches the relevant crossing allows us to predict the relative variation of the bond-forming and electron-transfer cross-sections as a function of collision energy. This calculation shows that, as we observe, the ratio of the yield of the bond-forming channel to the yield of electron transfer remains approximately constant as the collision energy is varied. The calculations also show that the ratio of chemical to electron-transfer yields in the D_2 collision system will be similar to that in the H_2 collision system, again as we observe experimentally. Obviously, if there is another surface that leads to the formation of the electron-transfer products which is not in direct competition with the bond-forming channel this will not be included in our calculation. However, since the variation with the collision energy of the crossing probability for any additional electron-transfer crossing should be similar to that of Eq. (8) the general insensitivity of the ratio of the bond-forming to electron-transfer yield to variations

in the collision energy should be unaffected, just the absolute value of the ratio. The qualitative agreement we find between the model in Fig. 4 and the results of our simplified Landau–Zener calculations lends further support to the general applicability for the surface crossing model for understanding dication reactivity.

The absolute product ion yields for HF^+ formation are given in Table 4. Correction of these yields for the discrimination effects of the TOFMS is not straightforward as the mechanism of formation of HF^+ is unclear. For example, we do not know if HF^+ is the forward or back-scattered product. The discrimination effects in the dication counts can be corrected (Table 4) but this correction does not significantly change the general trends of the data: an increase in the HF^+ signal with increasing collision energy. If the HF^+ is forward scattered, modelling shows that the trends in the data (Table 4) will not be dramatically changed by the correction for the energy discrimination of the TOFMS. Even if the HF^+ is back scattered, appropriate correction of the data in Table 4 then corresponds, within the approximations of the correction procedure, to an approximately constant, or slightly increasing, XF^+ absolute yield with collision energy. The possibility that the HF^+ product is back scattered is supported by the absence of any observable HF^+ signals in the first experimental investigation of the reactivity in this collision system, where back-scattered products were very inefficiently detected [11].

The energy dependence of the HF^+ product yield discussed before is markedly different to that observed for the other chemical product (HCF_2^+) in this collision system, strongly suggesting the two species derive from distinct chemical pathways. Perhaps the bifurcation in pathways occurs following the initial formation of an $[X_2–CF_3]^{2+}$ intermediate followed by hydrogen migration to form $[HF–CHF_2]^{2+}$, which have been proposed [7] as the first steps in the formation of XCF_2^+ from $CF_3^{2+} + X_2$. Analogous co-ordination then migration mechanisms have been proposed, supported by ab initio studies, for the reaction of both CF_2^{2+} and CO_2^{2+} with X_2 [6]. If the $[HF–CHF_2]^{2+}$ intermediate decays by cleavage of the C–FH bond, instead of cleavage of the F–H bond, which has been proposed [7] as the route to XCF_2^+, then HF^+ is formed. Such a mechanism has been shown to be consistent with the absence of an intramolecular isotope effect in the formation of XF^+ following collisions of CF_3^{2+} with HD [7].

Given the uncertainties in the detection efficiency of XF^+ it is hard to precisely quantify the branching ratio to form this product. However, this bond-forming channel is certainly much weaker, by approximately a factor of 50, than the formation of XCF_2^+.

6. Conclusions

The ionic products formed in collisions of CF_3^{2+} with X_2 (X = H, D) have been quantified as a function of the collision energy. The cross-section for forming CF_2^+ ions from electron-transfer reactions and the cross-section for the chemical reaction forming XCF_2^+ increase with decreasing collision energy and the ratio of these cross-sections is similar in both of the collision systems and does not vary strongly with energy. An additional chemical channel forming XF^+ is also detected. The markedly differing energy dependence of the cross-section for forming XCF_2^+ and XF^+ appear to indicate that these ions are formed via independent pathways.

Acknowledgements

NT thanks the EPSRC for the award of a studentship. This experiment was supported by the EPSRC under Grant GR/K11222. SDP thanks the Leverhulme Trust for a Research Fellowship. The authors would also like to thank Nik Kaltsoyannis for advice on theoretical methodology. This study is a part of the European Network RTN1-1999-00254 “Generation, Stability and Reaction Dynamics of Multiply Charged Ions” (MCInet).

References

[1] D. Schroder, H. Schwarz, J. Phys. Chem. A 103 (1999) 7385.
[2] D. Mathur, Phys. Rep. 225 (1993) 193.

[3] S.D. Price, J. Chem. Soc. Faraday Trans. 93 (1997) 2451.
[4] Z. Herman, Int. Rev. Phys. Chem. 15 (1996) 299.
[5] Z. Herman, J. Zabka, Z. Dolejsek, M. Farnik, Int. J. Mass Spectrom. 192 (1999) 191.
[6] L. Mrazek, J. Zabka, Z. Dolejsek, J. Hrusak, Z. Herman, J. Phys. Chem. A 104 (2000) 7294.
[7] N. Tafadar, D. Kearney, S.D. Price, J. Chem. Phys. 115 (2001) 8819.
[8] K.A. Newson, N. Tafadar, S.D. Price, J. Chem. Soc. Faraday Trans. 94 (1998) 2735.
[9] K.A. Newson, S.D. Price, Chem. Phys. Lett. 294 (1998) 223.
[10] K.A. Newson, S.D. Price, Chem. Phys. Lett. 269 (1997) 93.
[11] S.D. Price, M. Manning, S.R. Leone, J. Am. Chem. Soc. 116 (1994) 8673.
[12] P. Tosi, W.Y. Lu, R. Correale, D. Bassi, Chem. Phys. Lett. 310 (1999) 180.
[13] P. Tosi, R. Correale, W.L. Lu, S. Falcinelli, D. Bassi, Phys. Rev. Lett. 82 (1999) 450.
[14] W.Y. Lu, P. Tosi, D. Bassi, J. Chem. Phys. 112 (2000) 4648.
[15] Z. Dolejsek, M. Farnik, Z. Herman, Chem. Phys. Lett. 235 (1995) 99.
[16] B.K. Chatterjee, R. Johnsen, J. Chem. Phys. 91 (1989) 1378.
[17] N. Tafadar, N. Kaltsoyannis, S.D. Price, Int. J. Mass Spectrom. 192 (1999) 205.
[18] S.D. Price, M. Manning, S.R. Leone, Chem. Phys. Lett. 214 (1993) 553.
[19] N. Kaltsoyannis, S.D. Price, Chem. Phys. Lett. 313 (1999) 679.
[20] J. Hrusak, N. Sandig, W. Koch, Int. J. Mass Spectrom. 187 (1999) 701.
[21] W.C. Wiley, I.H. McLaren, Rev. Sci. Inst. 26 (1955) 1150.
[22] Y.Y. Lee, S.R. Leone, P.H. Champkin, N. Kaltsoyannis, S.D. Price, J. Chem. Phys. 106 (1997) 7981.
[23] S.D. Price, Y.Y. Lee, M. Manning, S.R. Leone, Chem. Phys. 190 (1995) 123.
[24] K. Yamasaki, S.R. Leone, J. Chem. Phys. 90 (1989) 964.
[25] S.D. Price, S.A. Rogers, S.R. Leone, J. Chem. Phys. 98 (1993) 9455.
[26] S.A. Rogers, S.D. Price, S.R. Leone, J. Chem. Phys. 98 (1993) 280.
[27] S. Lias, in: W. Mallard, P. Linstrom (Eds.), NIST Chemistry WebBook, NIST Standard Reference Database Number 69, National Institute of Standards and Technology, Gaithersburg, MD, 20899 (http://webbook.nist.gov), 2000.
[28] R.E. Olson, F.T. Smith, E. Bauer, Appl. Opt. 10 (1971) 1848.
[29] L. Landau, Phys. Z. Sowjetunion 2 (1932) 26.
[30] C. Zener, Proc. R. Soc. Lond. Ser. A 137 (1932) 696.
[31] E.C.G. Stueckelburg, Helv. Phys. Acta 5 (1932) 369.
[32] J. Hrusak, Z. Herman, N. Sandig, W. Koch, Int. J. Mass Spectrom. 201 (2000) 269.
[33] M.J. Frisch, G.W. Trucks, H.B. Schlegel, G.E. Scuseria, M.A. Robb, J.R. Cheeseman, V.G. Zakrzewski, R.E. Stratmann, J.C. Burant, S. Dapprich, J.M. Millam, A.D. Daniels, K.N. Kudin, M.C. Strain, O. Farkas, J. Tomasi, V. Barone, M. Cossi, R. Cammi, B. Mennucci, C. Pomelli, C. Adamo, S. Clifford, J. Ochterski, G.A. Petersson, P.Y. Ayala, Q. Cui, K. Morokuma, D.K. Malick, A.D. Rabuck, K. Raghavachari, J.B. Foresman, J. Cioslowski, J.V. Ortiz, B.B. Stefanov, G. Liu, A. Liashenko, P. Piskorz, I. Komaromi, R. Gomperts, R.L. Martin, D.J. Fox, T. Keith, M.A. Al-Laham, C.Y. Peng, A. Nanayakkara, C. Gonzalez, M. Challacombe, P.M.W. Gill, B. Johnson, W. Chen, M.W. Wong, J.L. Andres, C. Gonzalez, M. Head-Gordon, E.S. Replogle and J.A. Pople, Gaussian 98, Revision A.3, Gaussian, Inc., Pittsburgh, PA, 1998.
[34] J. Hrusak, Z. Herman, S. Iwata, Int. J. Mass Spectrom. 192 (1999) 165.
[35] P. Champkin, N. Kaltsoyannis, S.D. Price, Int. J. Mass Spectrom. Ion. Process 172 (1998) 57.
[36] D.V. Dearden, J.W. Hudgens, R.D. Johnson, B.P. Tsai, S.A. Kafafi, J. Phys. Chem. 96 (1992) 585.